Monolayer-Sensitive Infrared Imaging of DNA Stripes Using Apertureless Near-Field Microscopy

ARTICLE *in* LANGMUIR · JULY 2002

Impact Factor: 4.46 · DOI: 10.1021/la025700r

4 AUTHORS:

Boris B Akhremitchev
Florida Institute of Technology
55 PUBLICATIONS **1,253** CITATIONS
SEE PROFILE

Yujie Sun
Peking University
61 PUBLICATIONS **1,042** CITATIONS
SEE PROFILE

Larissa Stebounova
University of Iowa
27 PUBLICATIONS **448** CITATIONS
SEE PROFILE

Gilbert C. Walker
University of Toronto
172 PUBLICATIONS **4,971** CITATIONS
SEE PROFILE

Langmuir
The ACS Journal of Surfaces and Colloids

JULY 9, 2002
VOLUME 18, NUMBER 14

Letters

Monolayer-Sensitive Infrared Imaging of DNA Stripes Using Apertureless Near-Field Microscopy

Boris B. Akhremitchev, Yujie Sun, Larissa Stebounova, and Gilbert C. Walker*

Department of Chemistry, University of Pittsburgh, Pittsburgh, Pennsylvania 15260

Received March 5, 2002. In Final Form: May 16, 2002

Monolayer-sensitive chemical imaging with a lateral spatial resolution of approximately 200 nm is demonstrated. Apertureless near-field scanning infrared microscopy was employed to study samples patterned with regions of DNA and hexadecanethiol. The scattering of the infrared radiation was modulated by an oscillating metallic probe, and the scattered signal was demodulated at twice the probe's oscillation frequency. The maps of the near-field signal reveal patterns that are not readily observable in the topographic images, indicating the absence of topography-related artifacts. The decrease in the scattering from areas coated with 24 base pair long DNA molecules is attributed to a phosphate stretching absorption band. The near-field absorption is observed to be larger than the far-field absorption.

Introduction

Recent progress in near-field microscopy is stimulating a continuously growing interest in chemical imaging on the nanometer scale.[1−9] The apertureless type (sometimes called the scattering type) of near-field microscopy provides unsurpassed resolution for imaging over broad regions of the electromagnetic spectrum.[10−13] Vibrational sensitivity with 10^{-8}−10^{-7} m spatial resolution is achieved either *via* strong enhancement of the Raman signal that is enabled by using nanometer-sized antennae and electronic absorption of the sample[4] or by detecting the attenuation of scattered infrared radiation.[1,6,10,14] While Raman near-field microscopy provides high resolution and the possibility to measure the entire vibrational spectra of the molecules, its use is typically limited by very small nonresonant Raman cross sections and therefore the necessity to rely on electronic resonance enhancement of the cross section. By using infrared (IR) absorption it is possible to study samples without depending on electronic absorption, and this is particularly useful for studies of polymers and biomolecules. A prominent challenge has been to reduce the minimum detected number of absorbing chromophores. In this paper we report what we believe to be the first use of a near-field scanning infrared

* To whom correspondence may be addressed. E-mail: gilbertw@pitt.edu.

(1) Akhremitchev, B. B.; Pollack, S.; Walker, G. C. *Langmuir* **2001**, *17*, 2774−2781.
(2) Dragnea, B.; Leone, S. R. *Int. Rev. Phys. Chem.* **2001**, *20* (1), 59−92.
(3) Michaels, C. A.; Stranick, S. J.; Richter, L. J.; Cavanagh, R. R. *J. Appl. Phys.* **2000**, *88*, 4832−4839. Barbara, P. F.; Adams, D. M.; O'Connor, D. B. *Annu. Rev. Mater. Sci.* **1999**, *29*, 433−469.
(4) Stockle, R. M.; Suh, Y. D.; Deckert, V.; Zenobi, R. *Chem. Phys. Lett.* **2000**, *318*, 131−136. Hayazawa, N.; Inouye, Y.; Sekkat, Z.; Kawata, S. *Chem. Phys. Lett.* **2001**, *335*, 369−374. Nieman, L. T.; Krampert, G. M.; Martinez, R. E. *Rev. Sci. Instrum.* **2001**, *73*, 1691−1699.
(5) Azoulay, J.; Debarre, A.; Richard, A.; Tchenio, P. *Appl. Opt.* **2000**, *39*, 129−134.
(6) Hillenbrand, R.; Knoll, B.; Keilmann, F. *J. Microsc.* **2001**, *202*, 77−83.
(7) Maghelli, N.; Labardi, M.; Patane, S.; Irrera, F.; Allegrini, M. *J. Microsc.* **2001**, *202*, 84−93.
(8) Anderson, M. S. *Appl. Phys. Lett.* **2000**, *76*, 3130−3132.
(9) Hamann, H. F. *Z. Phys. Chem.* **2001**, *215*, 1025−1042.
(10) Lahrech, A.; Bachelot, R.; Gleyzes, P.; Boccara, A. C. *Appl. Phys. Lett.* **1997**, *71*, 575−577.
(11) Zenhausern, F.; O'Boyle, M. P.; Wickramasinghe, H. K. *Appl. Phys. Lett.* **1994**, *65*, 1623−1625.
(12) Knoll, B.; Keilmann, F. *J. Microsc.* **1999**, *194*, 512−515.
(13) Knoll, B.; Keilmann, F.; Kramer, A.; Guckenberger, R. *Appl. Phys. Lett.* **1997**, *70*, 2667−2669.
(14) Gresillon, S.; Ducourtieux, S.; Lahrech, A.; Aigouy, L.; Rivoal, J. C.; Boccara, A. C. *Appl. Surf. Sci.* **2000**, *164*, 118−123.

10.1021/la025700r CCC: $22.00
Published on Web 06/07/2002

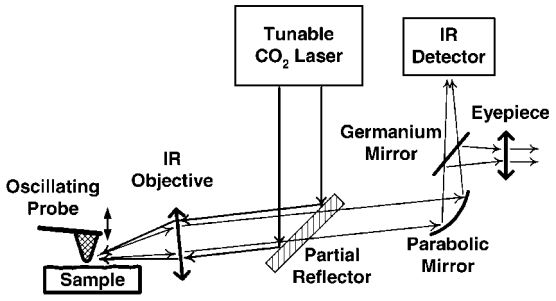

Figure 1. A schematic of the apertureless near-field infrared microscope.

microscopy to study the infrared absorption of a molecular monolayer, in this case a sub-monolayer of DNA.

Experimental Details

We use a home-built apparatus that is based on a commercial atomic force microscope (MultiMode AFM, Digital Instruments Inc., Santa Barbara, CA). The optical scheme of the instrument is shown in Figure 1. The IR radiation from a tunable carbon dioxide laser is directed toward a reflecting IR objective by a ZnSe partial (50/50) reflector (II-VI Inc., Saxonburg, PA). Radiation is focused by an IR objective (0.28 NA, Coherent Inc., Auburn, CA) onto the end of a platinum-coated cantilever probe, perpendicular to the long axis of the probe. We use p-polarized light with an ~80° angle of incidence. The spot size is approximately 50 μm, and the laser radiation power is 20−100 mW.

The probe is a commercial silicon probe (MikroMasch, Tallinn, Estonia) coated with 25 nm of platinum. To assist the focusing of the invisible CO_2 laser radiation, we co-propagate the IR beam with the visible radiation from a He−Ne laser prior to a partial reflector (the He−Ne laser is not shown in Figure 1). The IR radiation scattered by the probe and the sample propagates back through the same IR objective and the partial reflector. We use a paraboloidal mirror (effective focal length 127 mm, Janos Technology Inc., Townshend, VT) to focus the backscattered radiation onto a MCT infrared detector (Graseby Infrared, Orlando, FL). A germanium mirror in the path of the infrared radiation reflects the visible radiation, aiding in the visual inspection of the probe. All of the optical components described above, except the IR detector and the lasers, are rigidly attached on a platform, which is mounted atop an XYZ translational stage. The IR detector is mounted on a separate translational stage to enable adjustment of the position of the focused radiation on the sensing element. This design facilitates the tuning of the focused IR beam onto the end of the cantilever and the direction of collected radiation onto the detector. The electrical signal from the IR detector's preamplifier is further amplified by a lock-in amplifier (SR844, Stanford Research Systems Inc., Sunnyvale, CA) and collected by a computer, simultaneously with the atomic force microscopy (AFM) data. We used either the cantilever oscillation signal or the harmonic of this signal as reference signals in lock-in detection.

The far-field absorption spectra of DNA grafted onto gold substrates were collected with an FTIR spectrometer (Thermo Nicolet, Madison, WI) equipped with a specular reflection accessory (model 500, Spectra-Tech, Shelton, CT) tuned for a 75° angle of incidence. Bare, ungrafted gold-coated substrates were used to collect the reference spectra.

The patterned DNA samples were prepared as follows. Glass substrates were coated with gold (100 nm) by vacuum evaporation. Micro-contact printing[15] was employed to create stripes of 1-hexadecanethiol. The presence of ~5 μm wide stripes of 1-hexadecanethiol was confirmed by AFM topography imaging. Patterned gold substrates were incubated in a thiolated DNA solution (0.25 mM solution of 24-cytosine single-strand 3′-thiolated DNA oligomer in deionized water). After incubation, the substrates were cleaned of excess DNA by sonication in deionized water and dried in a stream of nitrogen gas. All samples were used within 2 days of preparation.

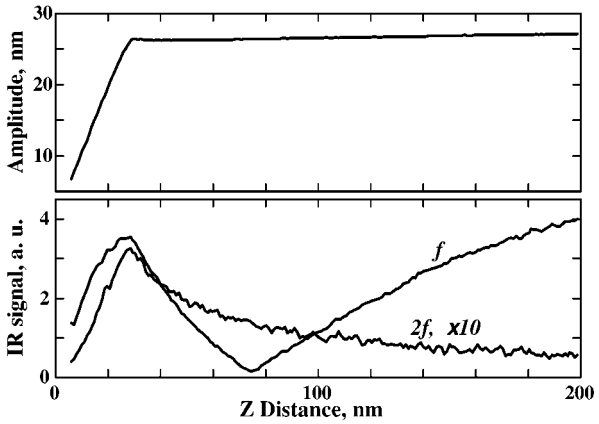

Figure 2. The top panel shows how the amplitude of the vertical probe oscillation depends on the separation from the surface. The bottom panel shows IR signals demodulated at the frequency of the probe oscillation (f) and twice the oscillation frequency ($2f$). The interferometric feature present in the f signal is missing from the $2f$ signal.

Results and Discussion

Modulation of the scattered radiation by oscillating a probe near the sample's surface is one of the most common features of detection of a near-field signal. Lock-in detection at the frequency of probe oscillation (f) is often used in order to filter the near-field signal from the large background. It has been noted that the distance dependence of such a signal is often nonmonotonic, which has been attributed to the interference of radiation from different sources.[1] In other words, the signal detected at frequency f might have a significant component that is not specific to the surface just under the tip. Due to the large spot size of the focused IR beam, a significant portion of the cantilever is illuminated, providing a background contribution to the detected scattered signal. The scattered signal that is detected at the cantilever oscillation frequency might have a significant component due to this background scattering. Detection of the scattered signal at the twice the frequency of the probe's oscillation provides a convenient way to extract the surface-specific signal.[7,16,17] It has been established that probe oscillation upon approach toward the surface remains harmonic (see, for example, ref 18); thus the presence of the second harmonic in the scattered signal indicates a strong nonlinearity in the near-field signal upon approach to the surface. A coupled-dipoles model[19] predicts a nonlinear polarizability modulation of the spherical tip of radius a and sample upon tip−sample separation r

$$\Delta\alpha \propto 1/(a^2 + r^2)^{3/2}$$

Figure 2 shows both the distance dependence of the cantilever oscillation amplitude (top panel) and the scattered IR signals, lower panel.

For brevity, we will call the signals that are collected at one and two times the frequency of the cantilever oscillation, the f and $2f$ signals, respectively. The $2f$ signal

(15) Xia, Y.; Whitesides, G. M. *Annu. Rev. Mater. Sci.* **1998,** *28*, 153−184.

(16) Wurtz, G.; Bachelot, R.; Royer, P. *Eur. Phys. J. Appl. Phys.* **1999**, *5*, 269−275.

(17) Knoll, B.; Keilmann, F. *Opt. Commun.* **2000**, *182*, 321−328.

(18) Anczykowski, B.; Gotsmann, B.; Fuchs, H.; Cleveland, J. P.; Elings, V. B. *Appl. Surf. Sci.* **1999**, *140*, 376−382.

(19) Zenhausern, F.; Martin, Y.; Wickramasinghe, H. K. *Science* **1995**, *269*, 1083−1085.

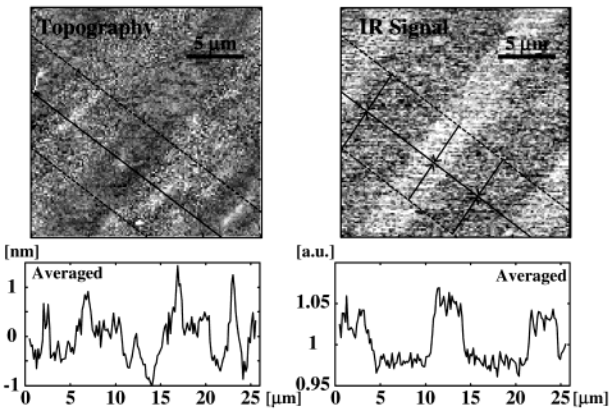

Figure 3. The image on the left shows the topography of the striped DNA−hexadecanethiol sample; the image on the right shows the 2*f* infrared signal. The 10 μm stripe pattern can be easily seen in the IR signal image; DNA regions are darker than alkanethiol regions. Several height features that are discernible in the topographic image are not coupled to the IR signal. Graphs below each image show the projection of the signal from a 7.5 μm wide area onto a line perpendicular to the linear pattern, as indicated in the corresponding images.

amplitude in Figure 2 has been multiplied by 10 for it to appear on the same graph as the *f* signal. It can be noted that in the region where the cantilever oscillation amplitude is relatively constant (30−200 nm from the surface), the 2*f* signal decreases monotonically with increasing tip−surface separation, while the *f* signal does not. Nonmonotonic dependencies can produce artifacts during imaging. At distances less than ∼30 nm, the amplitudes of both signals decay because of mechanical damping of the probe oscillation by the surface.

We have performed simultaneous topography and *2f* signal mapping of a surface patterned with alternating DNA and 1-hexadecanethiol stripes. Figure 3 shows two 20 μm × 20 μm images collected with a ∼100 nm peak-to-peak amplitude of tip oscillation at ∼133 kHz.

The near-field signal was acquired using 980 cm^{-1} radiation, which corresponds to the phosphate IR absorption band of DNA.[20] Lock-in detection at 2*f* (∼266 kHz) was accomplished with a 3 ms time constant. The scan rate was 0.3 Hz. The mean near-field 2*f* signal collected during scanning corresponds to ∼0.5 nW of IR radiation power incident on the detector, modulated at 2*f*. The striped pattern from the contact printed surface is visible in the topography image, although sharp edges of the DNA stripes are not readily discernible in this image. The near-field image shows a periodic variation corresponding to the periodicity and structure of the stamp that was used in the sample's preparation. From the images we see that the near-field map does not directly correlate with the topographic map; the cross-correlation coefficient between images is −0.15. Tip motion coupling into the near-field signal, also known as the "z-motion artifact",[21] is usually responsible for topographic artifacts in the constant gap scanning method that was employed here. Because there is a low correlation between the topography and the near-field signal in Figure 3, we conclude that the near-field signal is not topography-coupled. To compare signals in the regions covered with hexadecanethiol and DNA, we project signals from 7.5 μm wide areas, as indicated with dashed lines in the images, onto a line perpendicular to

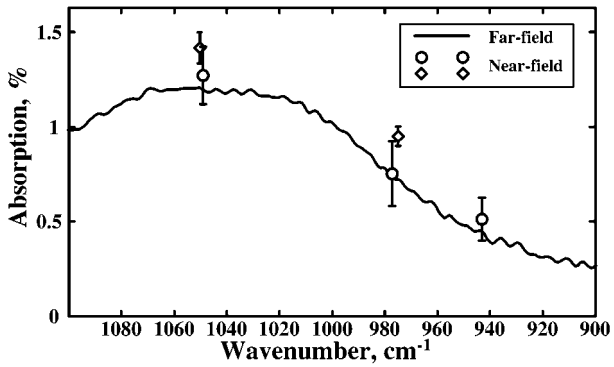

Figure 4. The graph shows the far-field IR absorption of a DNA monolayer grafted onto a gold substrate, in the spectral region of phosphate absorption band (continuous line). The figure also shows the result of averaging the near-field IR images at three different wavelengths (circle and diamond symbols). The different symbols for the near-field signal correspond to two different sets of measurements.

the direction of the linear pattern. Averaged topography and 2*f* signal graphs are shown below the corresponding images. These graphs convincingly demonstrate the absence of coupling between the near-field signal and the topography. We note that not all images of the patterned DNA sample that we have collected have such a low correlation between topography and 2*f* signal as the images in Figure 3. The highest degree of coupling corresponds to cross correlation between maps of approximately −0.5 (data not shown). Images with better-defined topography compared to that shown in Figure 3 indicate that the DNA layer is ∼2 nm thicker than hexadecanethiol layer. The small thickness of the DNA monolayer indicates that the DNA molecules are not closely packed on the surface and that the molecules extend from the surface by approximately half of their backbone length.

A line plot of the IR signal in Figure 3 shows that the 2*f* signal from the DNA monolayer is ∼7% weaker than the signal from the hexadecanethiol monolayer. This figure shows remarkably strong IR contrast for just one monolayer of molecules, though magnitude of this difference varies significantly from image to image collected under similar conditions. To obtain a mean value of the IR contrast, we have averaged images together at three different wavelengths of IR radiation in the phosphate backbone IR absorption region. Distinct topographic features were used to align the images during averaging. Figure 4 shows the IR contrast signal resulting from averaging the 2*f* signal at different wavelengths in five experiments and the far-field IR absorption spectrum of the DNA monolayer.

Averaging of many data files was necessary since the IR contrast varies from image to image. Factors affecting the contrast possibly include the history of the tip usage (shape deformation and/or contamination) and sample aging. From 6 to 35 images were combined in each experiment. We note a very broad and featureless far-field absorption band, characteristic of surface absorbed DNA;[22] the broad width of the phosphate band precluded measurement across the entire band because of the limited tunability of CO_2 laser. The averaging process used here reduces the microscope's sensitivity to small length-scale chemical heterogeneity. The near-field absorption follows the same wavelength dependence as the far-field absorption, further confirming that the contrast in our near-

(20) Taillandier, E.; Liquier, J. *Methods Enzymol.* **1992**, *211*, 307−335.

(21) Hecht, B.; Bielefeldt, H.; Inouye, Y.; Pohl, D. W.; Novotny, L. *J. Appl. Phys.* **1997**, *81*, 2492−2498.

(22) Boncheva, M.; Scheibler, L.; Lincoln, P.; Vogel, H.; Akerman, B. *Langmuir* **1999**, *15*, 4317−4320.

field images is caused by varying chemical composition. The averaged near-field absorption of DNA (∼1%) is approximately the same as far-field absorption, although the IR contrast in several experiments notably exceeded the far field absorption, as can be seen by comparing Figures 3 and 4. Near-field measurements were performed with p-polarized light, and we speculate that the direction of the IR electric field was nearly perpendicular to the direction of the asymmetric phosphate stretch transition dipole for the large fraction of phosphate groups, substantially decreasing the strength of the IR absorption. The enhanced IR absorption in the near-field could be related to the well-known phenomenon of surface-enhanced infrared absorption.[23] In our case the increase of absorption could be explained by an electric field enhancement[24,25] under the metallic tip. Alterations in the IR absorption strength could be due to tip shape modification or tip contamination during imaging.

We have estimated the resolution of monolayer-sensitive near-field IR imaging by examining the sharpness of the edge of the DNA absorption features; the resolution corresponds to approximately 200 nm (10−90% transition). It is likely that this resolution is worse than the limit attainable with our microscope and that with a higher signal-to-noise ratio the resolution could be approaching the size of the probe of ∼50 nm. The resolution achievable in apertureless near-field infrared microscopy is ∼15−30 nm and is limited by a combination of factors, such as the size of the probe and the scan height above the surface.[12,14] Also, an estimate of resolution using the edge width depends on actual sharpness of the features. We think that these factors explain why our estimated resolution is not as good as that obtained by others. An area with a diameter of 200 nm for ∼3 nm thick DNA monolayer corresponds to a signal from $\sim 5 \times 10^5$ phosphate groups ($\sim 10^{-18}$ mol). It is possible that the number of absorbing phosphate groups is much less due to DNA chain orientation and that our actual sensitivity is even higher.

Conclusions

We have demonstrated monolayer sensitivity in near-field scanning infrared microscopy by detecting contrast from a DNA/alkane patterned sample. Chemical contrast imaging was achieved by examining IR absorption in the spectral region of the phosphate stretching band of DNA molecules and harmonic demodulation of the signal scattered by the oscillating probe. IR absorption maps revealed that the IR signal was not coupled to vertical tip motion, indicating artifact-free imaging. We have observed a strong IR absorption from the regions grafted with DNA, and we speculate that the enhancement of the infrared absorption in our experiments has the same origin as the phenomenon of surface-enhanced infrared absorption. The observed contrast corresponds to detection of $\sim 10^{-18}$ mol of phosphate groups, with ∼200 nm lateral resolution. Technological advances in detecting the weak IR signal will provide even higher resolution and sensitivity.

Acknowledgment. We gratefully acknowledge support from ONR (N0001-96-1-0735), NSF (Phys-0103048 and CHE-9816820), and ARO (DAAD 16-99-C-1036).

LA025700R

(23) Osawa, M. *Top. Appl. Phys.* **2001**, *81*, 163−187.
(24) Martin, O. J. F.; Girard, C. *Appl. Phys. Lett.* **1997**, *70*, 705−707.
(25) Larsen, R. E.; Metiu, H. *J. Chem. Phys.* **2001**, *114*, 6851−6860.